Targeted Administration into the Suprachoroidal Space Using a Microneedle for Drug Delivery to the Posterior Segment of the Eye

Samirkumar R. Patel,[1] *Damian E. Berezovsky,*[2] *Bernard E. McCarey,*[2] *Vladimir Zarnitsyn,*[1] *Henry F. Edelhauser,*[2] *and Mark R. Prausnitz*[1]

Purpose. This study seeks to determine the intraocular pharmacokinetics of molecules and particles injected into the suprachoroidal space of the rabbit eye in vivo using a hollow microneedle.

Methods. Suprachoroidal injections of fluorescein and fluorescently tagged dextrans (40 and 250 kDa), bevacizumab, and polymeric particles (20 nm to 10 μm in diameter) were performed using microneedles in New Zealand white rabbits. The fluorescence intensity within the eye was monitored in each animal using an ocular fluorophotometer to determine the distribution of the injected material in the eye over time as compared with intravitreal injection of fluorescein. Fundus photography and histology were performed as well.

Results. Molecules and particles injected near the limbus using a microneedle flowed circumferentially around the eye within the suprachoroidal space. By targeting the suprachoroidal space, the concentration of injected materials was at least 10-fold higher in the back of the eye tissues than in anterior tissues. In contrast, intravitreal injection of fluorescein targeted the vitreous humor with no significant selectivity for posterior versus anterior segment tissues. Half-lives in the suprachoroidal space for molecules of molecular weight from 0.3 to 250 kDa ranged from 1.2 to 7.9 hours. In contrast, particles ranging in size from 20 nm to 10 μm remained primarily in the suprachoroidal space and choroid for a period of months and did not clear the eye. No adverse effects of injection into the suprachoroidal space were observed.

Conclusion. Injection into the suprachoroidal space using a microneedle offers a simple and minimally invasive way to target the delivery of drugs to the choroid and retina. (*Invest Ophthalmol Vis Sci.* 2012;53:4433–4441) DOI:10.1167/iovs.12-9872

From the [1]School of Chemical and Biomolecular Engineering, Georgia Institute of Technology, Atlanta, Georgia; and [2]Emory Eye Center, Emory University School of Medicine, Atlanta, Georgia.

Supported by National Eye Institute Grant R24-EY-017045 and an unrestricted grant from Research to Prevent Blindness.

Submitted for publication March 18, 2012; revised May 14, 2012; accepted May 30, 2012.

Disclosure: **S.R. Patel**, Clearside Biomedical (I, E), P; **D.E. Berezovsky**, None; **B.E. McCarey**, None; **V. Zarnitsyn**, Clearside Biomedical (I, E), P; **H.F. Edelhauser**, Clearside Biomedical (I, S), P; **M.R. Prausnitz**, Clearside Biomedical (I, S), P

Corresponding author: Mark Prausnitz, School of Chemical and Biomolecular Engineering, Georgia Institute of Technology, 311 Ferst Drive, Atlanta, GA 30332-0100; prausnitz@gatech.edu.

In the United States alone, more than 1.8 million individuals are afflicted by wet age-related macular degeneration (AMD) and more than 4.1 million with diabetic retinopathy. These diseases are leading causes of blindness in industrialized nations and prevalence rates of these diseases are expected to nearly double by 2020.[1,2] Only within the past decade have therapeutic agents become available to effectively manage these chorioretinal diseases.[3,4] As a result, effectively delivering therapeutic agents to disease sites in the posterior segment of the eye is critical to attaining treatment efficacy.

Currently, drugs are delivered to treat diseases of the choroid and retina by intravitreal administration. This is commonly done by injecting a liquid formulation into the vitreous, and more recently, placing extended-release implants in the vitreous.[5–7] However, it is often overlooked that the tissue site of action for many of these therapeutic agents is not the vitreous but the choroid and retina. As a result, a delivery method that can maintain therapeutic levels of a drug in the target tissues (i.e., choroid and retina) should provide more effective therapy for chorioretinal diseases.

This targeting can be accomplished by administering drugs into the suprachoroidal space (SCS). The SCS is a potential space located between sclera and choroid that can expand to accommodate a fluid or drug formulation. The location of the SCS adjacent to the target site for treatment of diseases like wet AMD and diabetic retinopathy may provide higher drug levels in the target tissues. For this reason, the SCS represents a promising new site of administration for treatment of posterior segment diseases and has become a recent focus of drug delivery research.[8–14]

Progress in this field, however, has been limited by the need for a reliable and minimally invasive way to access the SCS. Previous studies have accessed the SCS using surgical procedures that require a scleral incision and advancement of a long cannula or hypodermic needle through the SCS.[9–11] To improve on this cumbersome technique, we recently demonstrated injection into the SCS in cadaver eyes ex vivo using a hollow glass microneedle.[14]

Based on our previous in vitro study, this study assesses the goal of targeted administration to the SCS using a metal microneedle in vivo. We first determined the extent to which a suprachoroidal injection localized delivery to the SCS and then measured the pharmacokinetics of clearance from the SCS after injection. For the first time, this study presents pharmacokinetic measurements in the SCS as a function of molecular mass and particle size for model fluorescent compounds, fluorescently tagged bevacizumab and particles of 20 nm to 10 μm in diameter. Overall, this study shows that the suprachoroidal route of administration can provide targeted delivery to chorioretinal tissues of the eye using a minimally invasive microneedle device.

Methods

Metal microneedles were fabricated from 33-gauge needle cannulas (TSK Laboratories, Tochigi, Japan). The cannulas were shortened to approximately 750 μm in length and the bevel at the orifice was shaped using a laser (Resonetics Maestro, Nashua, NH). The microneedles were electropolished using an E399 electropolisher (ESMA, South Holland, IL) and cleaned with deionized water. Glass microneedles were fabricated from borosilicate micropipette tubes (Sutter Instrument, Novato, CA), as described previously.[15] A custom, pen-like device was designed to hold the glass microneedle.[14] A cap on the device allowed adjustment of the microneedle length to 750 μm. Both types of microneedles were sterilized using an AN74j Anprolene sterilizer (Anderson Products, Haw River, NC).

Several formulations were used for injection into the eye. Sodium fluorescein was prepared at 600 μg/mL for SCS injection and 6 μg/mL for intravitreal (IVT) injection (NaF, Sigma-Aldrich, St. Louis, MO). The higher concentration for SCS injection was used because, in an SCS injection, the NaF is in a thin region and trapped between tissues, making it harder to pick up the fluorescence signal. Dextrans of 40 kDa and 250 kDa tagged with fluorescein isothiocyanate (FITC, Sigma-Aldrich) were prepared at 1.5 mg/mL. Bevacizumab tagged with Alexa-Fluor 488 was dissolved in Hanks' Balanced Salt Solution (Mediatech, Manassas, VA) at a concentration of 1.5 mg/mL. Bevacizumab was labeled using an Alexa-Fluor labeling kit (Invitrogen, Carlsbad, CA) with 5:1 Alexa-Fluor 488: bevacizumab molar ratio. Particles of 20 nm, 500 nm, 1 μm, and 10 μm diameter (FluoSpheres, Invitrogen) were suspended in an aqueous medium at 2 weight % solids, except for the 10-μm particle suspension, which contained 0.2 weight % solids.

All experiments were carried out using New Zealand white rabbits and were approved by the Emory University Institutional Animal Care and Use Committee. Practices complied with the ARVO Statement for the Use of Animals in Ophthalmic and Vision Research. Animals were anesthetized with an intramuscular injection of ketamine and xylazine before injection of a formulation within the eye. Animals were euthanized with an injection of pentobarbital through the ear vein as necessary for histology.

The microneedle device was attached to a 1-mL syringe containing the formulation to be injected. For an SCS injection, the eyelids of the rabbit were pushed back and the microneedle was inserted into the sclera 3 to 5 mm past the limbus in the superior temporal quadrant of the eye. Injection of 50 μL took less than 15 seconds, with an additional time of 30 seconds allowed before removing the microneedle from the eye to prevent excessive reflux. Metal microneedles were used to inject 1- and 10-μm particles; all other materials were injected with a glass microneedle. Intravitreal injections were performed using a 30-gauge hypodermic needle. The opposing eye was not injected.

Measurement of fluorescence intensity within the rabbit eye was performed using an ocular fluorophotometer (Ocumetrics, Mountain View, CA). This system provides a one-dimensional scan of fluorescence intensity from the front to the back of the eye, as described previously.[16] No anesthesia was necessary for scanning. The pupil was dilated using drops of a 2.5% solution of phenylephrine hydrochloride (Baush & Lomb, Tampa, FL).

The fundus of the rabbit eye was imaged using a Genesis-D handheld digital retina camera with a 90-diopter lens (Kowa Optimed, Torrance, CA). Tropicamide (Baush & Lomb) was applied topically to dilate the pupil and the animal was imaged while under anesthesia.

Eyes were enucleated from the animal at the end of the experiment and fixed in 10% buffered formalin. Sections near the injection site were removed, placed in Optimal Cutting Temperature media (Sakura Finetek, Torrance, CA), and frozen under dry ice or liquid nitrogen, and were cryosectioned 10- to 30-μm thick. Slides were imaged under brightfield and fluorescence optics (Nikon E600, Melville, NY).

Results

Microneedle Injection Targets the SCS

Our first goal was to develop a simple procedure to insert a microneedle directly into the sclera of a live rabbit without the need for a surgical cut down and inject a liquid formulation into the SCS using a syringe. This procedure would allow minimally invasive injection into the SCS that could be accomplished within seconds. Our previous ex vivo studies suggested that a microneedle length of 700 to 800 μm would enable microneedle penetration to the base of the sclera, but not deeper, and thereby target the SCS.[14] We therefore fabricated microneedles of 750-μm length (Fig. 1). This enables the microneedle to be inserted perpendicularly across the sclera and target the SCS. In contrast, the use of a hypodermic needle would require a careful oblique insertion to localize the needle within the SCS.[8–11,13]

To provide a visual assessment of SCS targeting, India ink was injected into the rabbit eye in vivo using a microneedle. Figure 2A shows the normal anatomy of the rabbit eye, with the sclera on the outside (i.e., on the top in Fig. 2A) and the choroid, retina, and vitreous humor progressively deeper toward the interior. Figure 2B shows the same tissues after injection using a microneedle. As shown by the black India ink, the injection was highly localized within the SCS. The injection of 50 μL took approximately 15 seconds and the injection procedure took approximately 1 minute (see Supplementary Material and Supplementary Video 1, http://www.iovs.org/lookup/suppl/doi:10.1167/iovs.12-9872/-/DCSupplemental). The video demonstrates that a fluid injected into the SCS using this method can immediately spread circumferentially within the SCS and even reach as far back as the optic nerve. This confirmed that a microneedle can target the SCS of the rabbit eye in vivo.

We next compared the targeting ability of an SCS injection with that of an intravitreal injection. After injection of sodium fluorescein (NaF, 376 Da), we monitored NaF distribution along the central visual axis of the eye over time using an ocular fluorophotometer. The baseline scans, before injection of NaF, helped identify the location of ocular tissues based on endogenous tissue fluorescence. Figure 3A shows representative results of a baseline scan with the peaks demarcating the retina, lens, and cornea of the eye. The SCS is located just behind (i.e., to the left in Fig. 3A) the retina peak and the vitreous humor is the region between the retina and the lens.

The results show that an intravitreal injection of NaF produced a large peak at the site of injection in the vitreous

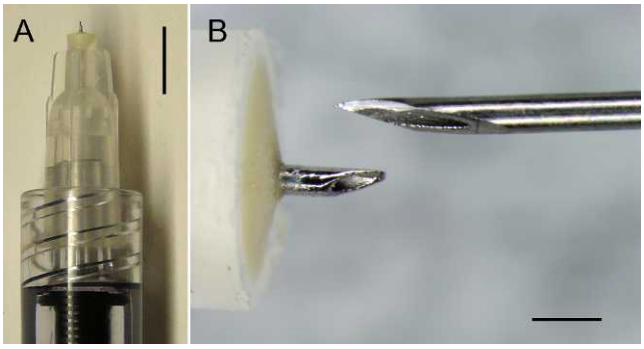

Figure 1. Microneedle for SCS injection. Low-magnification view of a microneedle at the end of a syringe (**A**) and high-magnification comparison of a microneedle (*left*) to the tip of a 30-gauge hypodermic needle (*right*). Scale bars: 5 mm (**A**) and 500 μm (**B**).

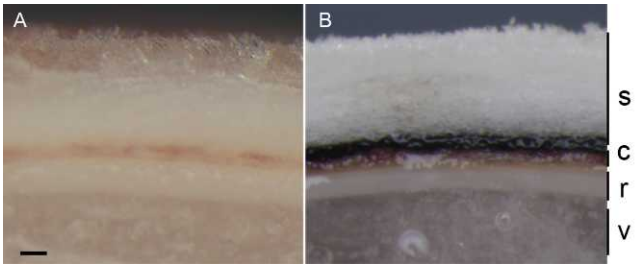

Figure 2. Frozen sections of an untreated rabbit eye (**A**) and a rabbit eye after injection of black India ink into the SCS (**B**) in vivo. The India ink can be seen between the sclera (s) and choroid (c) layers of the eye with the retina (r) and vitreous (v) below containing no ink. Scale bar: 100 μm.

humor within 30 minutes after injection (Fig. 3B). Within 1 to 2 hours, NaF distributed itself within the vitreous and generated a uniform concentration profile throughout the vitreous. The concentration of NaF decreased uniformly throughout the vitreous in the subsequent hours. Within 24 hours, NaF concentration in the eye returned to baseline levels, indicating NaF was no longer detectable. Using data in Figure 4A, the calculated half-life of NaF in the eye based on a first-order kinetic fit to the concentration within the mid-vitreous for each eye was 2.4 ± 0.2 hours (mean ± SD).

Injection of NaF in the SCS resulted in dramatically different distribution within the eye. Within 5 minutes after injection, a sharp concentration peak developed in the posterior segment of the eye (Fig. 3C). The location of this peak represents the SCS, since it is just posterior to the retina. Over time, this peak remained in the same location with significantly lower concentrations in the vitreous region, indicating targeting to the SCS. Similar to an intravitreal injection, within 24 hours, the NaF concentration throughout the eye returned to baseline levels, indicating the NaF had cleared the eye. Using data in Figure 4A, the calculated half-life of NaF based on a first-order kinetic fit to the concentration within the SCS for each eye was 1.2 ± 0.1 hours. No significant levels of NaF were detected in the anterior chamber or in any regions of the opposing uninjected eye from either route of administration (data not shown).

To quantify whether either route was effective at targeting the posterior tissues, we calculated the chorioretinal selectivity of each injection of NaF. We define the chorioretinal selectivity as the ratio of the concentration of NaF at the target chorioretinal tissues (i.e., between 16 and 24 on the x-axis of Fig. 3) to the concentration present at the vitreous/lens interface (i.e., between 80 and 90 on the x-axis). As shown in Figure 5, the ratio for an IVT injection is approximately at or below 1 for all times post injection. This indicates that NaF distributed throughout the vitreous region relatively evenly and there was little or no chorioretinal selectivity after intravitreal injection. This is consistent with a visual examination of the profiles in Figure 3B, which show relatively uniform concentrations throughout the vitreous.

In contrast, the chorioretinal selectivity 5 minutes after an SCS injection jumped to more than 200, indicating a strong selectivity for the chorioretinal region (Fig. 5). This selectivity decreased over time but always remained above 10. Chorioretinal selectivity was higher after SCS injection at all time points when compared with IVT injection (ANOVA, $P < 0.05$). This result demonstrates that SCS administration of NaF is much more effectively targeted to the chorioretinal tissues as compared with intravitreal injection.

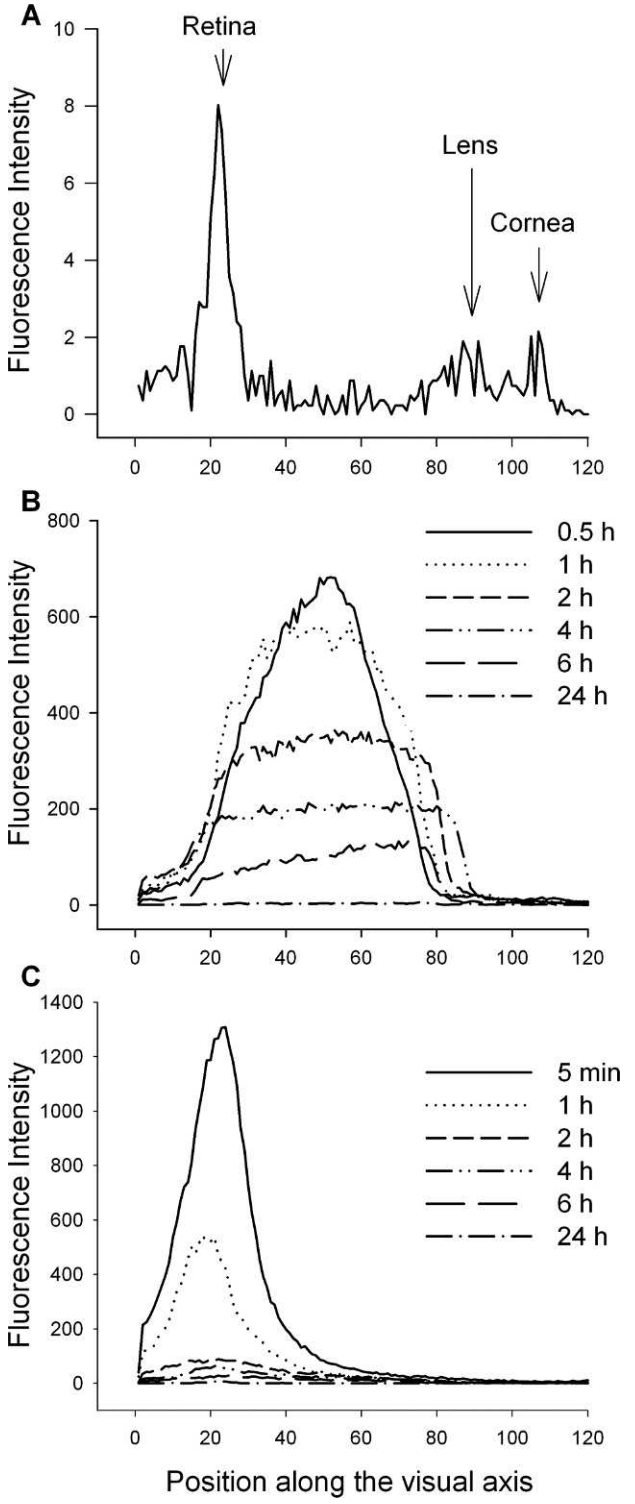

Figure 3. Fluorescence scans along the visual axis of the rabbit eye in vivo. A baseline scan of an untreated eye (**A**) delineates the retina, lens, and cornea of the eye owing to their natural background fluorescence. Intravitreal injection of NaF (**B**) caused an increase in the fluorescence intensity primarily within the vitreous that distributes uniformly throughout the vitreous and decays over time. Injection of NaF into the SCS (**C**) caused a sharp peak near the retina with a dramatically different profile than intravitreal injection. The NaF levels declined over a few hours and returned to baseline levels within 24 hours after both injections. Representative data are shown from three eyes at each condition.

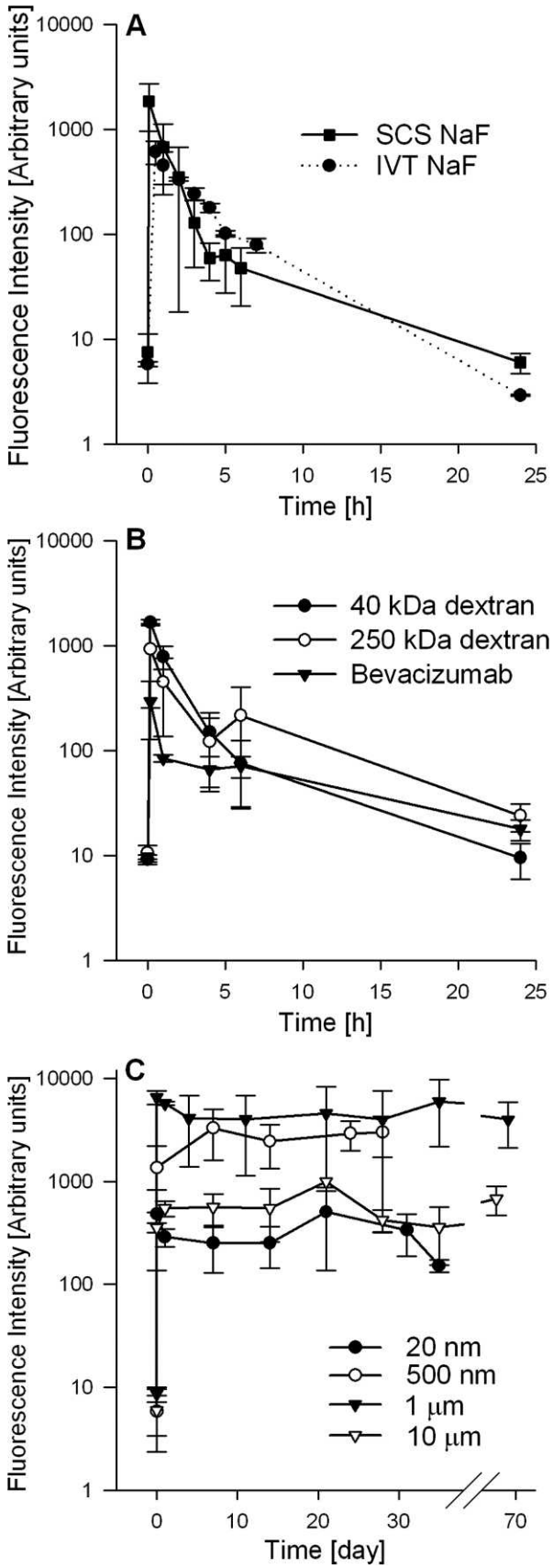

Figure 4. Pharmacokinetic profiles showing the clearance of molecules and particles from the rabbit eye in vivo. Peak fluorescence intensity in the SCS after SCS injection and peak fluorescence intensity in the vitreous after IVT injection of NaF (**A**). Peak fluorescence intensity in the SCS after SCS injection of fluorescently tagged macromolecules (**B**) and nano- and microparticles (**C**). Data points represent average (±SD), $n = 2$–3.

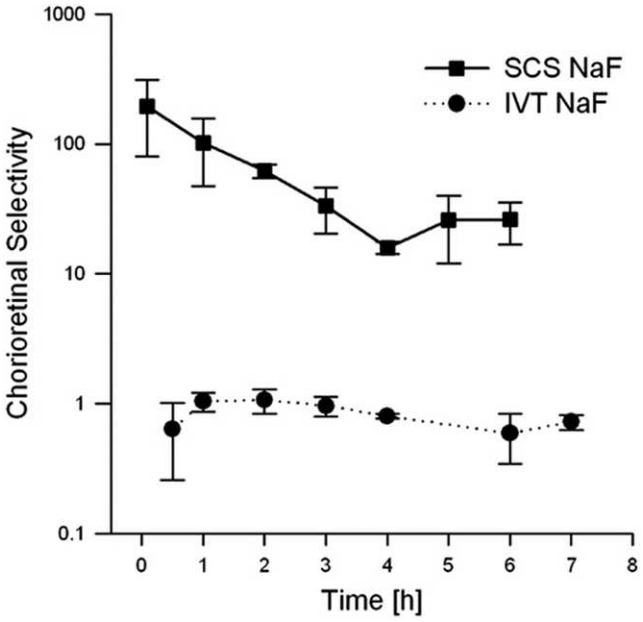

Figure 5. A comparison of the targeting of NaF to the choroid and retina resulting from SCS administration versus IVT injection in the rabbit eye in vivo. The chorioretinal selectivity is defined as the ratio of fluorescence intensity observed at the choroid and retina over what is observed at the lens. SCS administration of NaF resulted in at least an order of magnitude higher chorioretinal selectivity as compared with IVT injection. Data points represent average (±SD), $n = 3$.

Targeting of Macromolecules within the SCS

To determine if SCS injection also targets macromolecules to the chorioretinal region, we injected fluorescently tagged model compounds, 40 kDa and 250 kDa dextrans, as well as fluorescently tagged bevacizumab (Avastin) into the SCS.

For each of these three macromolecules, the distribution profiles after SCS injections were similar in shape to NaF, exhibiting a sharp peak in the SCS with a steep drop off in surrounding regions (Fig. 6). Over time, the peak value decreased, but maintained its overall shape and localization. At 24 hours, the fluorescence intensity of the 40-kDa dextran had reached near-baseline levels and the fluorescence of the 250-kDa dextran and tagged bevacizumab were slightly above baseline levels, indicating that the macromolecules were primarily cleared from the SCS within 1 day. Using data in Figure 4B, the calculated half-lives of 40-kDa dextran, 250-kDa dextran, and tagged bevacizumab in the SCS were 3.6 ± 0.5, 5.6 ± 1.0, and 7.9 ± 0.5 hours (mean ± SD), respectively.

Within 15 minutes after injection, the chorioretinal selectivity was at or above 100 for all three compounds and remained well above 10 throughout the experiment (Fig. 7A). This indicates that the injection was accurately targeted to the SCS and that these macromolecules remained highly localized in the chorioretinal tissues after injection.

Targeting of Particles within the SCS

We found that molecules in this study were cleared from the SCS within 1 day, which may not be long enough for most therapies. Sustained-release strategies have been developed for

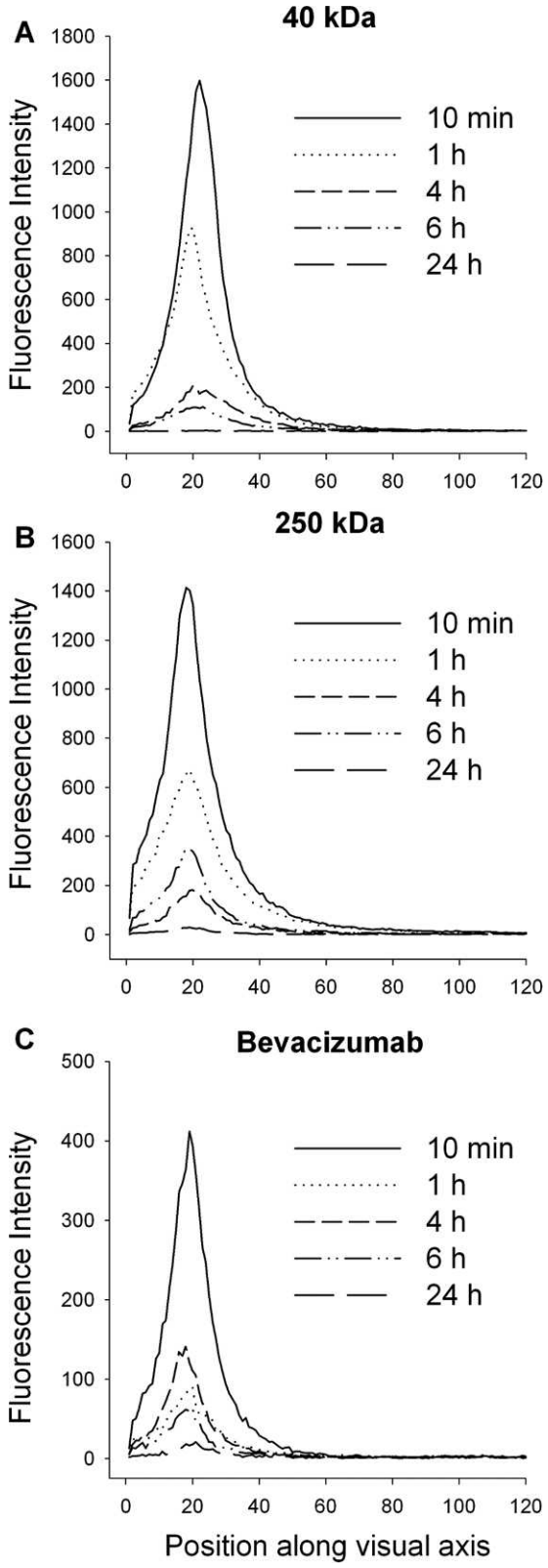

Figure 6. Fluorescence scans along the visual axis of the rabbit eye in vivo after administration of fluorescently tagged macromolecules in the suprachoroidal space. Model compounds, 40 kDa (**A**) and 150 kDa (**B**) dextran were injected using a microneedle into the SCS. Bevacizumab (**C**), a 147-kDa antibody, was also injected. All three injections resulted in a sharp fluorescent peak near the retina, indicating localization in the suprachoroidal space (see Fig. 1). The levels declined over a few hours and returned to near baseline levels within 24 hours after the injection. Representative data are shown from two to three eyes at each condition.

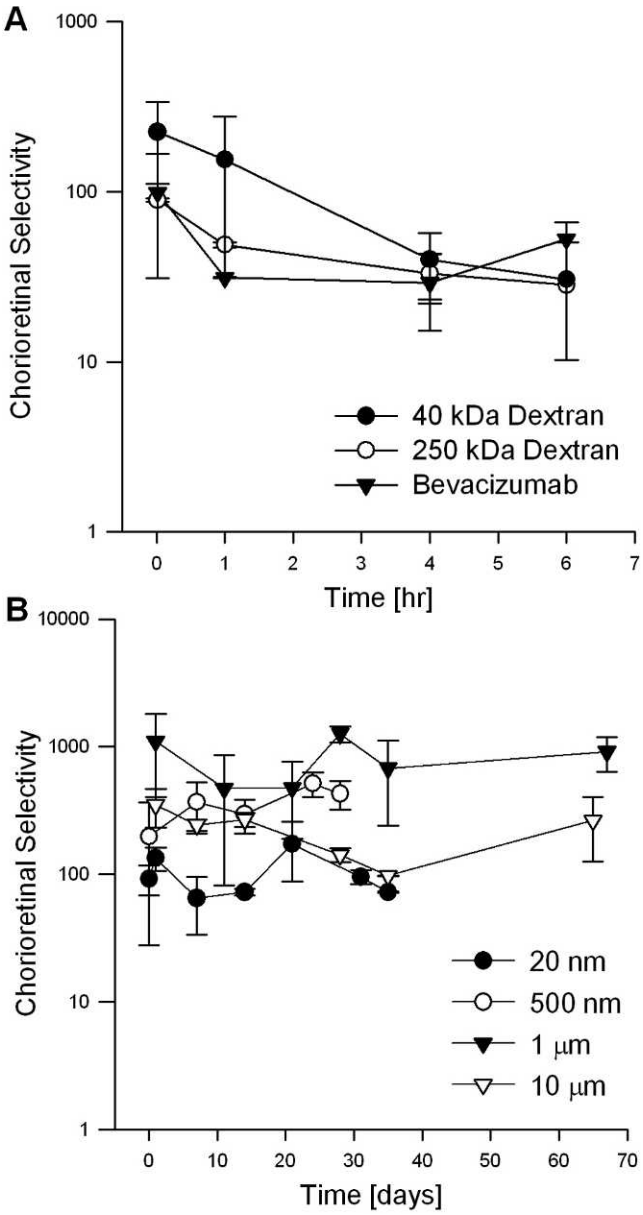

Figure 7. A comparison of the targeting of macromolecules (**A**) and particles (**B**) to the choroid and retina resulting from SCS administration in the rabbit eye in vivo. The chorioretinal selectivity is defined as the ratio of fluorescence intensity observed at the choroid and retina over what is observed at the lens. SCS administration of these materials results in a selectivity above 10 for the time periods tested. Data points represent average (±SD), $n = 2$–3.

other drug delivery scenarios using slow release of drug encapsulated within polymeric implants.[6,17] It would be clinically beneficial to inject a drug formulation that would release a drug over a 3- to 6-month period with a near zero-order drug-release profile. We therefore evaluated if particles injected into the SCS could be localized and remain there for months. If so, this would suggest that particles encapsulating drugs for slow release could be localized in the SCS to enable extended drug therapy. However, injection and distribution of particles of different sizes in the SCS have not been studied before.

We injected particles of 20 nm, 500 nm, 1 μm, and 10 μm diameter into the SCS of rabbit eyes in vivo and measured their fluorescence concentration as a function of position and time

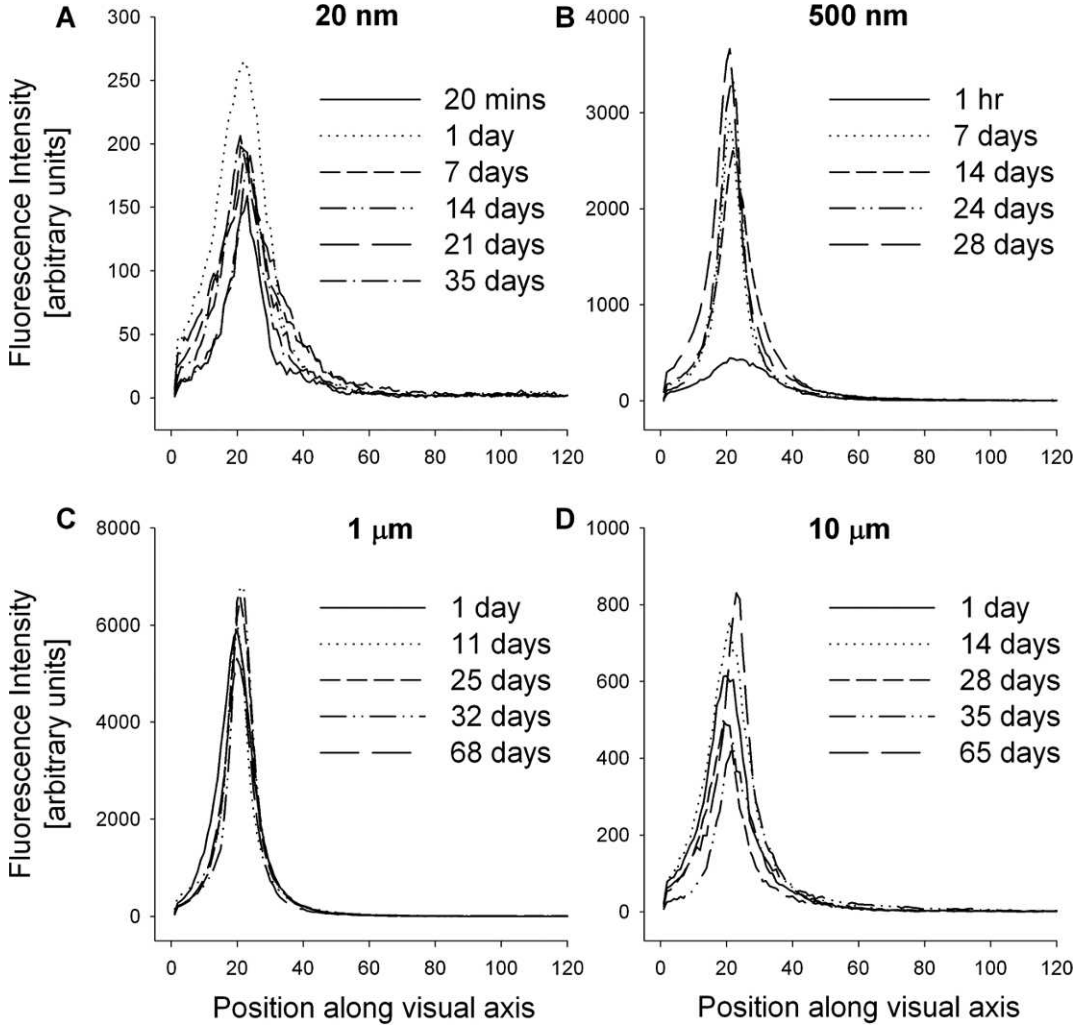

Figure 8. Fluorescence scans along the visual axis of the rabbit eye in vivo after administration of fluorescent particles in the suprachoroidal space. Four different-sized particles were injected: 20 nm (**A**), 500 nm (**B**), 1 μm (**C**), and 10 μm (**D**). All four particle injections resulted in a sharp fluorescent peak near the retina, indicating localization in the suprachoroidal space (see Fig. 1). The peak levels did not drop over the time tested, indicating the particles were still present for 1 to 2 months. Representative data are shown from two to three eyes at each condition.

using a protocol similar to the NaF experiments. Because our goal was to determine the distribution and lifetime of particles in the SCS, we used nondegradable particles labeled with a permanent fluorescent tag. We hypothesize that if nondegradable particles remain localized in the SCS for a long time, then similarly, degradable particles can degrade and release encapsulated drug according to their design without premature clearance from the SCS.

For all four of the particles examined, the distribution profiles after SCS injection showed the characteristic shape featuring a sharp peak in the SCS within minutes after injection (Fig. 8). The fluorescence intensity decreased sharply outside the SCS region, indicating that the particles had not significantly migrated into the surrounding tissues or the vitreous humor.

Unlike molecules, which were cleared relatively quickly from the SCS, the particles remained in the SCS for months. All rabbits maintained fluorescence intensity levels within the SCS similar to levels obtained immediately following suprachoroidal injection (Fig. 4C, ANOVA, $P > 0.25$). There appears to be no mechanism to clear these particles from the SCS, at least on the time scale of 1 to 2 months. Even the smallest particles of 20-nm diameter showed no decrease in fluorescence intensity.

Immediately after suprachoroidal injection, all particles had chorioretinal selectivity ratios of approximately 100 or greater (Fig. 7B). Over time, this selectively did not significantly change (ANOVA, $P > 0.05$). This shows that particles can be effectively targeted to the chorioretinal region and remain targeted for months.

To supplement fluorophotometry measurements, we also performed in vivo fundus imaging as well as histological examination at 2 months after SCS injection of 10-μm particles to provide visual confirmation of the presence of the particles in the SCS. Fundus photography provided a two-dimensional image of the posterior segment of the eye. The fundus of the injected eyes (Figs. 9A, 9C) appears normal with no inflammation or abnormalities as compared with an uninjected eye (Fig. 9E). Fluorescence images of the fundus revealed that the microparticles were distributed throughout the back of the eye and had reached the optic nerve (Figs. 9B, 9D). The fluorescence images of the fundus also show that particles are behind the choroidal blood vessels, as evidenced by blood vessels blocking some of the fluorescence. This confirms that even after 2 months, the particles were still present in the SCS.

To confirm the exact location of the particles, histological examination of the tissues was performed after the animals

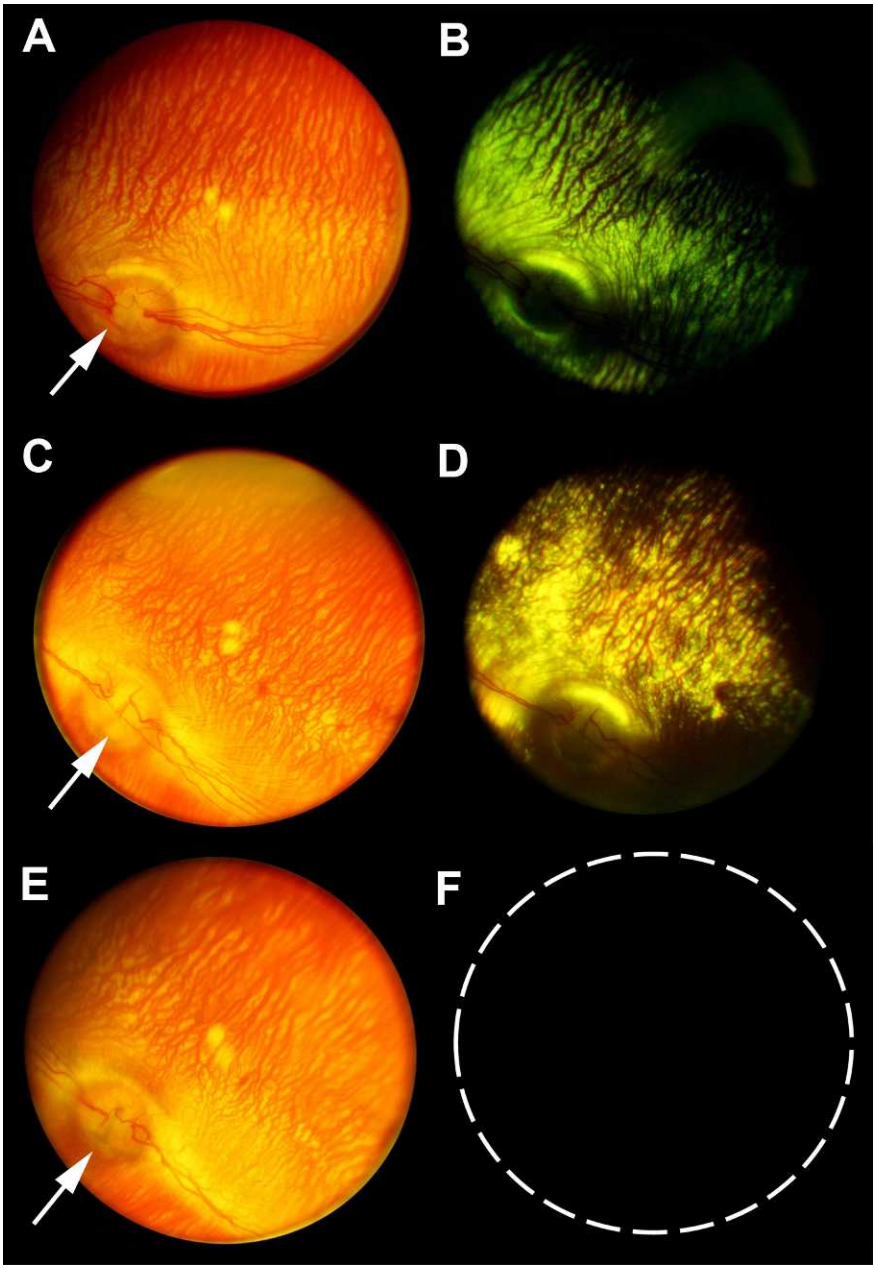

Figure 9. Images of the fundus of the rabbit eye in vivo 2 months after injection of 1 μm (**A**, **B**) and 10 μm (**C**, **D**) fluorescent particles in the SCS. The color image of the back of the eye (**A**, **C**) appears similar to an untreated eye (**E**). The arrow points to the optic cup, indicating the image is of the far back of the eye. The particles are clearly present in the SCS 2 months after injection since they show up under fluorescence imaging (**B**, **D**) behind choroidal blood vessels.

were killed at the end of the study and the eye was enucleated. Figure 10 shows a representative cross section of tissue 2 months after injection of 10-μm particles. This image shows the particles are selectively located in the SCS and choroid. The histology visually confirms the presence of particles in the SCS after 2 months and supports the quantitative fluorescence data.

Safety of Microneedle Injection into the SCS

Injections into the SCS using microneedles were well tolerated and no injection-related complications were observed. No bleeding occurred in any of the injections. Within 1 hour after each injection, the needle insertion site was no longer visible and in general the eye appeared indistinguishable from a naive eye. Fundus imaging of the rabbit eyes revealed no retinal detachment or choroidal vasculature changes in the posterior segment, even 2 months after injection of particles into the SCS. In all suprachoroidal injections, no apparent vision loss was observed in the rabbits.

Discussion

With the recent success of therapeutics to treat chronic chorioretinal diseases, it is clear that a safe, reliable, and practical way to administer these compounds to the back of the eye will be integral to the management of these diseases. Currently, the clinician's only practical way to deliver therapeutic agents to the posterior segment is to administer

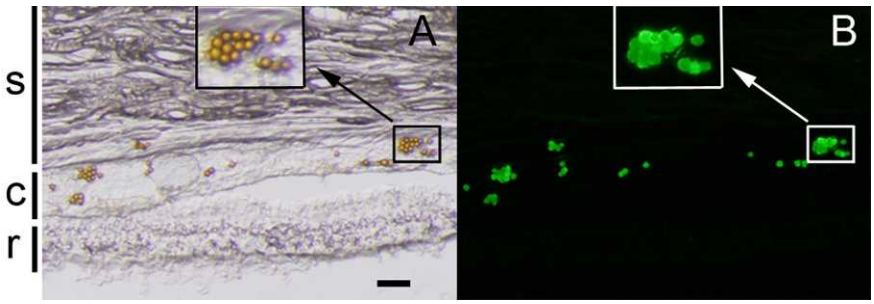

Figure 10. Histological cross-sections of rabbit eye tissue after SCS administration of 10 μm fluorescent particles. A brightfield (**A**) and fluorescence (**B**) microscopy image of particles 2 months after a SCS injection. The particles can be distinctly located in the lower sclera or choroid layers of the eye. The inset shows a blow up of the boxed region where individual particles can be seen. Scale bar: 100 μm.

the drugs into the vitreous, and this option has seen widespread use only in the past decade. Offering additional alternatives to intravitreal administration that target the diseased tissues would provide clinicians more options in managing chorioretinal diseases.

This work shows that suprachoroidal injections may be a viable option and using a microneedle could make this route of administration safe and simple. We showed in this study that injection with a microneedle can easily access the SCS and inject a variety of molecules and even nanoparticles and microparticles. We showed that particles, 10 nm to 10 μm, injected into the SCS do not appear to be cleared from the eye. Furthermore, we showed enhanced selectivity to the chorioretinal tissues after SCS injection characterizing the distribution profile of these materials in the eye.

The enhanced targeting enabled by suprachoroidal administration could lead to two distinct advances. First, it should result in higher drug levels in the target site, the chorioretinal tissues, compared with IVT injection at the same dose. As a consequence, delivery to the SCS may enable more accurate dosing and dose sparing. Second, targeting the SCS should decrease exposure of nontarget tissues to the drug. This would be advantageous when delivering drugs, such as steroids, that can cause side effects, including cataracts and increased IOP due to unintended drug diffusion to the lens and anterior segment of the eye.[18–20] These potential clinical benefits make suprachoroidal delivery particularly attractive.

This study also revealed that the clearance of molecules and particles injected into the SCS occurs at different rates. Small soluble molecules, as well as macromolecules, exhibited half-lives in the SCS on the order of hours, whereas suspensions of nano- and microparticles remained in the SCS for months with no sign of clearance. This suggests the existence of a sieving effect associated with clearance from the SCS that allows molecules as large as approximately 10 nm (i.e., the effective radius of gyration of the largest macromolecule used in this study, 250-kDa dextran,[21] but blocks particles with a diameter as small as 20 nm (i.e., the smallest nanoparticle used in this study). The flexibility of the dextran molecule to alter its shape may have also influenced its ability to be cleared, in contrast to the more-rigid nanoparticles. In addition to size, factors such as lipophilicity, charge, and other physiochemical properties may also play a role.

Clearance from the SCS could occur via passive diffusion across the sclera, uptake into choroidal capillaries, and flow through scleral channels near the vortex veins. We previously showed that sieving in the sclera occurs only for larger particles (i.e., diameter $>$ 500 nm),[14,15] which suggests that clearance from the SCS is not primarily via the sclera. Sieving by the choroidal capillary walls of the blood-retina barrier has been shown to exclude molecules larger than 3 to 6 nm in animal studies,[22,23] which is similar to the sieving cutoff observed here, albeit somewhat smaller. Thus, capillary drainage may play a role in clearance from the SCS. Finally, fluid outflow through scleral channels near the vortex veins has previously been observed in monkeys[24] and we have observed this in our in vitro studies too,[14] although no information about possible sieving in this pathway is available.

Independent of mechanism, the sieving effect suggests that biodegradable particles encapsulating drug could be used for sustained delivery from within the SCS. Because there does not appear to be a clearance mechanism for intact particles, degradable particles should remain in the SCS until the particle has broken down into polymer fragments that can be cleared, during which time encapsulated drug can be released from the particles over time. In this way, suprachoroidal injection of drug-loaded particles could enable sustained drug delivery to the chorioretinal tissues for as short as a day or as long as several months, based on drug release and particle degradation kinetics. Additional studies examining how formulation affects intraocular pharmacokinetics should help define optimal formulations for SCS injection.

The hollow microneedle design introduced in this study enabled minimally invasive access to the SCS. The microneedle design was versatile enough to allow injection of small molecules as well as particles up to 10 μm in size. By recognizing that the resistance to flow in the expandable SCS is much lower than through the relatively incompressible surrounding tissues, the microneedle did not need to physically enter the SCS or open it by blunt dissection. Instead, fluid injected from the microneedle naturally flowed into the SCS in seconds and expanded it anatomically. In contrast, the only other reported methods of accessing the SCS have used a cannula, which must be navigated into the SCS, or a hypodermic needle that is inserted parallel to the ocular surface. Both of these alternate methods require a surgical cut down of the sclera and involve physical contact with the choroid, both of which introduce risks of infection and choroidal bleeding, respectively.[9] The use of a microneedle should cause less trauma to the eye, because the needle tract is much shorter and narrower compared with other approaches, and can provide a straightforward way to access the SCS that could move this administration route from a surgical setting to a clinical office. Further studies will be needed to refine microneedle device development and to test suprachoroidal delivery in human eyes.

Acknowledgments

We thank Rinku Baid and Uday Kompella for providing Alexa-Fluor–labeled Avastin, Lennart Berglin and Louise Bergman for help with India ink injections, and Donna Bondy for administrative support. This work was carried out at the Institute for Bioengineering and Bioscience and the Center for Drug Design,

Development, and Delivery at the Georgia Institute of Technology and at the Emory Eye Center. SRP, VZ, HFE, and MRP are inventors on patents and have a significant financial interest in a company that is developing microneedle-based products for ocular delivery. This potential conflict of interest has been disclosed and is being managed by Georgia Tech and Emory University.

References

1. Friedman DS, O'Colmain B, Tomany SC, et al. Prevalence of age-related macular degeneration in the United States. *Arch Ophthalmol*. 2004;122:564–572.
2. Saaddine JB, Honeycutt AA, Narayan KM, Zhang X, Klein R, Boyle JP. Projection of diabetic retinopathy and other major eye diseases among people with diabetes mellitus: United States, 2005-2050. *Arch Ophthalmol*. 2008;126:1740–1747.
3. Chappelow AV, Kaiser PK. Neovascular age-related macular degeneration: potential therapies. *Drugs*. 2008;68:1029–1036.
4. Peyman GA, Lad EM, Moshfeghi DM. Intravitreal injection of therapeutic agents. *Retina*. 2009;29:875–912.
5. Kuno N, Fujii S. Biodegradable intraocular therapies for retinal disorders: progress to date. *Drugs Aging*. 2010;27:117–134.
6. Lee S, Hughes P, Ross A, Robinson M. Biodegradable implants for sustained drug release in the eye. *Pharm Res*. 2010;27: 2043–2053.
7. Yasukawa T, Ogura Y. Medical devices for the treatment of eye diseases. *Handb Exp Pharmacol*. 2010;469–489.
8. Kim SH, Galban CJ, Lutz RJ, et al. Assessment of subconjunctival and intrascleral drug delivery to the posterior segment using dynamic contrast-enhanced magnetic resonance imaging. *Invest Ophthalmol Vis Sci*. 2007;48:808–814.
9. Olsen TW, Feng X, Warner K, et al. Cannulation of the suprachoroidal space: a novel drug delivery methodology to the posterior segment. *Am J Ophthalmol*. 2006;142:777–787.
10. Einmahl S, Savoldelli M, D'Hermies F, Tabatabay C, Gurny R, Behar-Cohen F. Evaluation of a novel biomaterial in the suprachoroidal space of the rabbit eye. *Invest Ophthalmol Vis Sci*. 2002;43:1533–1539.
11. Hou J, Tao Y, Jiang YR, Wang K. In vivo and in vitro study of suprachoroidal fibrin glue. *Jpn J Ophthalmol*. 2009;53:640–647.
12. Gilger BC, Salmon JH, Wilkie DA, et al. A novel bioerodible deep scleral lamellar cyclosporine implant for uveitis. *Invest Ophthalmol Vis Sci*. 2006;47:2596–2605.
13. Olsen TW, Feng X, Wabner K, Csaky K, Pambuccian S, Cameron JD. Pharmacokinetics of pars plana intravitreal injections versus microcannula suprachoroidal injections of bevacizumab in a porcine model. *Invest Ophthalmol Vis Sci*. 2011;52:4749–4756.
14. Patel SR, Lin AS, Edelhauser HF, Prausnitz MR. Suprachoroidal drug delivery to the back of the eye using hollow microneedles. *Pharm Res*. 2011;28:166–176.
15. Jiang J, Moore JS, Edelhauser HF, Prausnitz MR. Intrascleral drug delivery to the eye using hollow microneedles. *Pharm Res*. 2009;26:395–403.
16. Ghate D, Edelhauser HF. Ocular drug delivery. *Expert Opin Drug Deliv*. 2006;3:275–287.
17. Kuppermann B. Implants can deliver corticosteroids, pharmacological agents. *Retina Today*. 2007;27–31.
18. Ozkiris A, Erkilic K. Complications of intravitreal injection of triamcinolone acetonide. *Can J Ophthalmol*. 2005;40:63–68.
19. Holekamp NM, Thomas MA, Pearson A. The safety profile of long-term, high-dose intraocular corticosteroid delivery. *Am J Ophthalmol*. 2005;139:421–428.
20. Razeghinejad MR, Katz LJ. Steroid-induced iatrogenic glaucoma. *Ophthalmic Res*. 2011;47:66–80.
21. Ambati J, Canakis CS, Miller JW, et al. Diffusion of high molecular weight compounds through sclera. *Invest Ophthalmol Vis Sci*. 2000;41:1181–1185.
22. Brubaker RF, Pederson JE. Ciliochoroidal detachment. *Surv Ophthalmol*. 1983;27:281–289.
23. Bill A, Sperber G, Ujiie K. Physiology of the choroidal vascular bed. *Int Ophthalmol*. 1983;6:101–107.
24. Pederson JE, Gaasterland DE, MacLellan HM. Experimental ciliochoroidal detachment. Effect on intraocular pressure and aqueous humor flow. *Arch Ophthalmol*. 1979;97:536–541.